Published in final edited form as:
Cancer Chemother Pharmacol. 2009 January ; 63(2): 303–312. doi:10.1007/s00280-008-0740-8.

NSC606985, a novel camptothecin analog, induces apoptosis and growth arrest in prostate tumor cells

Chen Tan,
Department of Medicine/Endocrinology, Weill Medical College of Cornell University, 1300 York Avenue, Box-149, Room F-233, New York, NY 10021, USA

Li-Qun Cai,
Department of Medicine/Endocrinology, Weill Medical College of Cornell University, 1300 York Avenue, Box-149, Room F-233, New York, NY 10021, USA

Wendy Wu,
Department of Medicine/Endocrinology, Weill Medical College of Cornell University, 1300 York Avenue, Box-149, Room F-233, New York, NY 10021, USA

Yaming Qiao,
Department of Medicine/Endocrinology, Weill Medical College of Cornell University, 1300 York Avenue, Box-149, Room F-233, New York, NY 10021, USA

Julianne Imperato-McGinley,
Department of Medicine/Endocrinology, Weill Medical College of Cornell University, 1300 York Avenue, Box-149, Room F-233, New York, NY 10021, USA

Guo-Qiang Chen, and
Department of Pathophysiology and Key Laboratory of Cell Differentiation and Apoptosis of Chinese Ministry of Education, Shanghai Jiao-Tong University School of Medicine, Shanghai, China

Yuan-Shan Zhu
Department of Medicine/Endocrinology, Weill Medical College of Cornell University, 1300 York Avenue, Box-149, Room F-233, New York, NY 10021, USA

Yuan-Shan Zhu: yuz2002@med.cornell.edu

Abstract

Purpose—Prostate cancer is a major cause of cancer mortality in American males. Once prostate cancer has metastasized, there is currently no curative therapy available. The development of effective agents is therefore a continuing effort to combat this disease. In the present study, the effects and potential mechanisms of NSC606985 (NSC), a water-soluble camptothecin analog, in prostate cancer cells were investigated.

Methods—Prostatic tumor cells, DU-145, LNCaP and PC-3, were used for the study. Cell proliferation, cell cycle, cell apoptosis and caspase 3/7 activity were determined in the presence or absence of NSC. The levels of Bax and Bak, and the release of cytochrome *c* from mitochondria were analyzed by Western blot.

Results—Treatment with NSC at nanomolar concentrations produced a time- and dose-dependent decrease in viable cell numbers of multiple prostate cancer cells. In DU-145 cells, NSC

Correspondence to: Yuan-Shan Zhu, yuz2002@med.cornell.edu.

produced a time-and dose-dependent induction of cell apoptosis and cell cycle arrest as evidenced by cell morphological changes, increases in S-phase and sub-G1 cell fractions, an elevation of caspase 3/7 activity, DNA fragmentation and apoptotic cells. NSC increased the levels of apoptotic proteins, Bax and Bak, and induced a release of cytochrome *c* from mitochondria to cytosol in DU-145 cells. Co-administration of Z-VAD-FMK, a pan-caspase inhibitor, blocked NSC-induced caspase 3/7 activity and cell apoptosis without affecting NSC-induced cell cycle arrest. In contrast, co-administration of a PKCδ inhibitor, rottlerin, had no significant effect on NSC induction of caspase activity, and slightly potentiated NSC-induced cell death. Furthermore, like camptothecin, a mutation of topoi-somerase 1 that prevents the binding of camptothecin to the enzyme completely abolished the NSC effect in DU-145 cells.

Conclusion—The data obtained suggest that NSC is able to decrease cell growth, induce cell apoptosis and cause growth arrest in prostatic tumor cells, which may involve an interaction with topoisomerase 1 and an activation of mitochondrial apoptotic pathway.

Keywords

Prostate cancer; Camptothecin analog; Apoptosis; Topoisomerase 1; Mitochondria

Introduction

Prostate cancer is a leading cause of cancer mortality in American and Western European males [1–3]. Once prostate cancer has metastasized, it is ultimately fatal for there is currently no curative treatment available [4, 5]. The major treatment, androgen deprivation therapy, is often only palliative and rarely curative. The tumor cells ultimately develop resistance to anti-androgen therapy and continue to metastasize. Chemotherapy has been used for the treatment of prostate cancer for years. However, the chemotherapeutic regimens used previously have little or no impact on the disease process [5, 6]. Recent efforts in chemotherapy with new agents and new combinatorial regimens have made significant progress, and improved the median survival in advanced prostate cancer patients [7, 8].

Camptothecins, as a promising new class of anticancer drugs, have advanced to the forefront of therapeutic and developmental chemotherapy, when either used alone or in combination. The demonstration of topoisomerase 1 (Top1) as the molecular target of camptothecins and the development of water-soluble derivatives with less side effects have translated this class of drugs into agents in the treatment of cancer [9–12]. Two water-soluble camptothecin analogs have been approved by The Food and Drug Administration for clinical application: topotecan, as a second-line therapy for ovarian cancer or small-cell lung cancer, and irinotecan, for the treatment of colorectal carcinoma refractory to 5-fluorouracil or as initial therapy in combination with 5-flurouracil for the treatment of metastatic colorectal cancer [11]. NSC606985 (NSC), a highly water-soluble camptothecin analog, has rarely been studied for its anticancer activity. Recent studies indicate that NSC can target other cellular molecular targets in addition to Top1 to display its anticancer activity. For example, NSC has been shown to inhibit HIF-1 induced gene transcription in transfection assays and hypoxia-induced VEGF gene expression in tumor cells [13].

We have recently shown that NSC produces a novel and differential effect in leukemic cells. In NB4 and U937 leukemic cells, NSC induces a proteolytic activation of PKCδ, resulting in a PKCδ-mediated caspase-dependent and a caspase-independent cell death; whereas, in K562 leukemic cells, it inhibits cell growth without activation of PKCδ and cell apoptosis [14]. In the current study, we investigated the effect and potential mechanisms of NSC in prostate cancer cells. The results obtained suggest that the anti-tumor activity of NSC in prostate cancer cells involves the interaction with Top1 and an activation of the

mitochondrial apoptotic pathway. It warrants further investigation as a potential therapeutic agent for the treatment of hormone-refractory prostate cancer.

Materials and methods

Reagents

NSC606985 (NSC, glycine, 4-ethyl-3,4,12,14-tetrahydro-3,14-dioxo-1H-pyrano[3′,4′:6,7]indolizino[1,2-b]quinolin-4-yl ester, (S)-, monohydrochloride, $C_{22}H_{19}N_3O_5 \cdot ClH$) was kindly provided by the Drug Synthesis and Chemistry Branch, Developmental Therapeutic Program, Division of Cancer Treatment and Diagnosis, National Cancer Institute (Bethesda, MD, USA). Tissue culture medium, rottlerin, paclitaxel, complete protease inhibitors and propidium iodide were obtained from Sigma (St Louis, MO, USA). Fetal bovine serum (FBS), L-glutamine, penicillin and streptomycin were from Gemini Bio-Products (Calabasas, CA, USA). Z-VAD-fluoromethylketone (Z-VAD-FMK), RNase A and protease K were from Promega (Madison WI). Antibodies against Bax and Bak were from Santa Cruz biotechnology (Santa Cruz, CA, USA), specific cytochrome ***c*** antibody (clone 7H8.2C12) from Pharmingen (San Diego, CA, USA), COX subunits IV antibody from Molecular Probes (Eugene, OR, USA), and *α*-tubulin antibody from Sigma.

Cell cultures

DU-145 (ATCC, Rockville, MD, USA), DU-145RC0.1 and DU-145 RC1 (kindly provided by Dr. Pommier, NIH) were grown in Dulbecco modified Eagle's minimal essential medium, LNCaP and PC-3 cells (ATCC) in RPMI-1640 medium supplemented with 10% FBS, 2 mM L-glutamine, 50 units/ml of penicillin and 50 μg/ml of streptomycin. Cells were maintained in a 5% CO_2-95% air humidified atmosphere at 37°C, and cultured in phenol-red free medium with 5% stripped FBS (Gemini Bio-Products, Calabasas, CA, USA) 24 h before experiments as described [15].

Cell proliferation and caspase 3/7 activity assays

For the determination of viable cell numbers and caspase 3/7 activity, prostate cancer cells were plated in 96-well plates at a density of approximately 40%, and treated with various drug regimens as indicated in the experiment 24 h after plating. The number of viable cells was determined using CellTiter AQueous One Solution Cell Proliferation Assay kit, and the caspase 3/7 activity, a common pathway in cell apoptosis, was determined using the Caspase-Glo 3/7 Assay kit from Promega (Madison, WI, USA) following the manufacturer's instruction.

Flow cytometry analysis of DNA Content and cell apoptosis

Approximately 1×10^6 cells were plated in 60-mm plates and treated with or without various concentrations of NSC in the presence or absence of 20 μM of Z-VAD-FMK or various doses of rottlerin for the times as indicated in the experiments. At the end of treatment, cells were collected, and analyzed for nuclear DNA content distribution and cell apoptosis. For DNA content analysis, cells were washed with phosphate buffered saline (PBS) and fixed with 70% ethanol for 1 h. The cells were centrifuged at 300*g* for 5 min, pellet washed twice with cold PBS, suspended in 500 μl PBS and incubated with 5 μl RNase (20 μg/ml final concentration) at 37°C for 30 min. The cells were then chilled over ice for 10 min and stained with propidium iodide (PI, 50 μg/ml final concentration) for 1 h, and analyzed by flow cytometry with a FACScan (Becton Dickinson, Germany). For flow cytometric analysis of cell apoptosis, cells were stained with Annexin V in combination with PI using the Annexin V-FITC apoptosis detection kit I from BD Pharmingen (San Diego, CA, USA) according to the manufacturer's instruction.

Determination of DNA fragmentation

The fragmented DNA was visualized by DNA-agarose gel electrophoresis followed by ethidium bromide staining as described [16]. Briefly, NSC treated and untreated cells were harvested and incubated in a lysis buffer [50 mmol/l Tris–HCl (pH 8.0), 20 mmol/l ethylenediamine tetra-acetic acid (EDTA), 10 mmol/l NaCl, 1% sodium dodecylsulfate (SDS)] for 20 min on ice. The samples were then centrifuged and treated with DNase-free RNase A and proteinase K. Following phenol and chloroform extraction, DNA was precipitated by ethanol and dissolved in 1 × Tris–EDTA buffer. DNA fragmentation was analyzed in a 2% agarose gel, visualized by ethidium bromide staining and photographed under ultraviolet light.

Western blot analysis

Western blot was carried out following standard method as previously described with minor modifications [17]. Briefly, cells were harvested and total cellular proteins were extracted using a lyses buffer (62.5 mM Tris–HCl pH 6.8, 100 mM dithiothreitol (DTT), 2% SDS, 10% glycerol). The protein concentrations were determined using the Bio-Rad Protein Assay following the manufacturer's instruction (Bio-Rad, Hercules, CA, USA). Equal amounts of proteins were fractionated on a 15% SDS-PAGE, and transferred to PVDF membrane (Amersham Pharmacia Biotech, Piscata-way, NJ, USA). The blots were blocked with TBST buffer [500 mM NaCl, 20 mM Tris–HCl (pH 7.4), and 0.1% Tween 20] containing 5% nonfat dry milk and then incubated with specific primary antibody in TBST buffer containing 5% nonfat dry milk (Bio-Rad Laboratories, Hercules, CA, USA) overnight at 4°C. Following secondary antibody incubation, the signal was visualized using the SuperSignal West Pico Chemiluminescent kit (Pierce Biotechnology Inc., Rockford, IL, USA), and exposed to Kodak X-Max film. α-Tubulin was used as an internal control by incubating a specific antibody against α-tubulin with the same membrane following stripped off.

Analysis of cytochrome *c* release

The detection of cytochrome *c* release from mitochondria to cytosol was performed as previously described with minor modifications [18]. Briefly, harvested cells were pelleted by centrifugation and resuspended in 5× volumes of Buffer A [20 mM HEPES, 10 mM KCl, 1.5 mM $MgCl_2$, 1 mM EDTA, 1 mM ethylene glycol bis(β-aminoethyl ether)-N,N,N′,N′-tetraacetic acide (EGTA), 1 mM DTT, 0.1 mM phenylmethylsulfonyl fluoride (PMSF), and complete protease inhibitors] supplemented with 250 mM sucrose. The samples were incubated on ice for 30 min, and then homogenized in a Teflon homogenizer. The samples were fractionated by three sequential centrifugations of 1,000*g*, 10,000*g*, and 20,000*g*. The pellet obtained at 10,000*g* was considered as the "mitochondrial" fraction and the supernatant at 20,000*g* as the cytosol fraction. The fractionated proteins were analyzed by Western blot in a 15% SDS-PAGE as described above.

Statistics

The data are presented as mean ± SEM. One-way analysis of variance (ANOVA) following post hoc Student-Newman–Keuls test was used to determine the difference among multiple groups. A *P* value less than 0.05 was considered statistically significant.

Results

NSC decreased viable cell numbers in multiple prostate cancer cells

To determine whether NSC is effective in inhibiting cell growth, the number of viable cells was determined in multiple prostate cancer cell lines after treatment with NSC. As shown in

Fig. 1, treatment with NSC produced a time- and dose-dependent decrease in viable cell numbers in multiple prostate cancer cell lines, including hormone-sensitive LNCaP cells, and hormone-independent DU-145 and PC-3 cells. At a dose of 50 nM, NSC caused a more than 50% reduction of viable cell numbers after 72 h treatment compared to the original cell numbers in DU-145 cells (Fig. 1a). Similar NSC effects were observed in PC-3 cells (Fig. 1b). However, LNCaP cells were less sensitive to NSC, and the decrease in viability at 72 h was not so obvious when compared to the original cell number (Fig. 1c). As a positive control, treatment with vinblastine (VBT), a cell mitotic inhibitor, at 0.1 μg/ml concentration for 72 h significantly decreased viable cell number in all prostate cancer cells (Fig. 1c; [15]).

NSC induced cell apoptosis and cell cycle arrest

To determine whether NSC induced decreases in viable cell number is associated with cell apoptosis, the NSC effect on apoptosis was analyzed in DU-145 and LNCaP cells. As shown in Fig. 2a–d, treatment with NSC in DU-145 cells produced dose- and time-dependent morphological changes that were characteristics of apoptosis such as chromatin condensation and nuclear fragmentation with intact cell membrane. Analysis of nuclear DNA distribution using flow cytometry showed that NSC induced a time- and dose-dependent increase in hypoploid cells (sub-G1 cells). The fraction of sub-G1 cells, an important indication of apoptotic cells, was increased from 2.1% in control DU-145 cells to 3.0, 20.3 and 27.6% in cells treated with NSC (50 nM) for 24, 48 and 72 h, respectively. This NSC induction of sub-G1 cells was completely blocked by the concomitant administration of Z-VAD-FMK (20 μM), a pan-caspase inhibitor [19]. The fraction of S-phase cells was increased from 18.41% in control DU-145 cells to 38.58, 34.14 and 36.27% in cells treated with NSC (50 nM) for 24, 48 and 72 h (see Fig. 2e–h), respectively. This NSC induced cell cycle arrest in DU-145 cells was not affected by the concomitant administration of Z-VAD-FMK (20 μM) as shown in Fig. 2i–l.

Annexin-V/PI staining was performed to determine early, late apoptotic and necrotic cells following NSC treatment in DU145 cells. Treatment with NSC at a 50 nM concentration in DU145 cells produced a time-dependent increase in early (annexin V^+/PI^-) and late apoptotic or necrotic cells (annexin V^+/PI^+) as shown in Fig. 3a–f. The fractions of annexin V^+/PI^- and annexin V^+/PI^+ cells were increased from 4.68 and 1.01% in control to 13.43 and 13.9% in NSC (50 nM) treated cells for 72 h, respectively. Co-administration of Z-VAD-FMK (20 μM) greatly blocked the NSC induced apoptosis (Fig. 3g–j). In contrast, the addition of rottlerin (1 μM) slightly potentiated the NSC induced apoptosis and cell death (Fig. 3k–l). Actually, treatment with rottlerin alone also increased cell apoptosis and cell death in DU-145 cells. NSC induced cell apoptosis was further supported by demonstrating that NSC (50 nM) produced a time-dependent induction of DNA fragmentation (Fig. 3o), a land marker of cell apoptosis.

In LNCaP cells, NSC induced a time-dependent cell cycle arrest with a modest increase in cell apoptosis. Upon NSC treatment at 50 nM, the fraction of S-phase cells in cell cycle analysis was increased from 6.3% in control to 12.2, 12.7 and 13.5% in cells treated with NSC for 24, 48, and 72 h, respectively; the fraction of early apoptotic cells (annexin V^+/PI^-) in annexin V/PI staining was increased from 0.7% in control to 3.9, 4.7, and 5.7%; and the fraction of late apoptotic and necrotic cells (annexin V^+/PI^+), from 1.6% in control to 4.6, 4.4 and, 7.0% at 24, 48 and 72 h of treatment, respectively (data not shown).

NSC produced a dose- and time-dependent induction of caspase activity

As shown in Fig. 4, treatment with NSC produced a time-and dose-dependent induction of caspase 3/7 activity in DU–145 cells. Treatment with NSC for 4 h did not alter the caspase 3/7 activity. However, the caspase 3/7 activity was significantly increased at 24 h of NSC

treatment at a dose of 50 nM, and further elevated after 48 h of treatment. This NSC-induced increase in caspase activity was completely blocked by the co-administration of Z-VAD-FMK (20 μM), a pan-caspase inhibitor. Whereas, the addition of rottlerin, a PKCδ inhibitor, failed to inhibit the NSC action while it slightly potentiated the NSC-induced caspase activity at 1 μM of rottlerin at 48 h. These changes in caspase activity were parallel to the changes in cell apoptosis as shown in Figs. 2 and 3. As a positive control, cells treated with paclitaxel (100 nM), a microtubule-interacting agent that induces apoptosis via activation of caspases [20], also showed a significant increase in caspase 3/7 activity at 48 h of treatment, which was blocked by Z-VAD-FMK.

NSC treatment increased Bax and Bak levels and caused cytochrome *c* release from mitochondria to cytosol in DU-145 cells

Treatment with NSC at 50 nM for 24 h in DU-145 cells produced a more than twofold induction of Bax and Bak, two pro-apoptotic factors related to the mitochondrial apoptotic pathway, which were not affected by the co-administration of Z-VAD-FMK as shown in Fig. 5a and b, as they are in the upstream of caspase activation in the mitochondrial apoptotic pathway.

To determine whether cytochrome ***c*** was released from mitochondria into cytosol in NSC-treated cells, cytosolic and mitochondrial fractions of proteins were prepared from NSC-treated DU-145cells, and analyzed by Western blot. As shown in Fig. 5c, NSC induced a time-dependent accumulation of cytochrome ***c*** in the cytosol with a simultaneous reduction in the mitochondrion. Cox IV, an inner membrane molecule of mitochondria, used as a marker of mitochondrial fraction, was not detected in the cytosol.

The NSC actions were blocked by a pan-caspase inhibitor, but not a specific PKCδ inhibitor in DU-145 cells

As a previous study [14] indicates that NSC-induced apoptosis involves PKCδ activation in leukemic cells, the involvement of PKCδ in NSC-induced apoptosis and cell growth inhibition was tested in DU-145 cells using a specific PKCδ inhibitor, rottlerin [21]. As shown in Fig. 6, rottlerin failed to modulate the NSC-induced decrease in viable cell numbers although rottlerin itself caused a dose-dependent inhibition of cell growth. Similarly, rottlerin did not block the NSC-induced caspase activity (Fig. 4) and slightly potentiated NSC-induced apoptosis (Fig. 3). On the other hand, co-administration of Z-VAD-FMK, a pan-caspase inhibitor, with NSC significantly rescued cell growth (Fig. 6), as well as completely blocked the NSC-induced caspase 3/7 activity (Fig. 4) and cell apoptosis (Figs. 2, 3). As a positive control, treatment with paciltaxel at 100 nM significantly decreased the number of viable cells (Fig. 6) while induced the caspase activity (Fig. 4), which were significantly blocked by the co-administration of Z-VAD-FMK.

Top1 mutation abolished the NSC effects

To determine whether the NSC-induced cell growth inhibition involves the interaction with Top1 in DU-145 cells, DU-145RC0.1 and DU-145RC1, two cell lines derived from DU-145 cells that are resistance to camptothecin due to a Top1 mutation that abolishes the binding of camptothecin to top1 [22], were treated with various doses of NSC for 72 h. As shown in Fig. 7, both NSC and camptothecin failed to decrease the numbers of viable cells in these Top1 mutated cells although they produced a dramatic effect in the parental DU-145 cells. However, paclitaxel, a cytotoxic agent by acting on microtubules, was as effective in the Top1 mutated DU-145RC0.1 cells as in the parental DU-145 cells.

Discussion

Camptothecins have become a rapidly growing family of anticancer agents with a wide-spectrum anticancer activity and impressive in vivo efficacy as exemplified by the two FDA-approved drugs: topotecan and irinotecan. In the present study, we have demonstrated that NSC, a rarely studied and water-soluble camptothecin analog, produced a dose-and time-dependent inhibition of cell growth and promotion of cell apoptosis and cell cycle arrest in multiple prostate cancer cells as evidenced by the determination of viable cell numbers, examination of cell morphology, flow cytometric analyses**,** detection of cytochrome ***c*** release from mitochondria to cytosol, and analyses of caspase activity and DNA fragmentation. Similar to our observation in leukemic cells [14], NSC produced a cell differential effect, i.e., in DU-145 cells, it caused dramatic cell apoptosis and growth arrest, while it mainly induced growth arrest in LNCaP cells. Although previous studies have shown that camptothecin and its analogs may interact with various molecular targets such as inhibition of HIF-1 induced gene transcription, hypoxia-induced VEGF gene expression [13, 23], and activation of PKCδ [14], our current study in DU-145 cells suggests that the primary target of NSC is Top1, resulting in DNA damage, and an activation of apoptotic pathway.

Top1 plays an essential role in cell metabolism and survival and it is a primary target of camptothecins [10, 12, 24]. The conventional role of human Top1 comprises of the relaxation of DNA supercoiling and relief of torsional strain during DNA processing, including replication, transcription and repair. Competothecin stabilizes the covalent top1-DNA cleavage complex by reversibly blocking top1-mediated DNA religation and free top1 release, and thus leaves the DNA with a protein-linked DNA single-strand break, which triggers DNA damage, cytotoxic lesions and cell apoptosis as well as cell cycle arrest in the G2/M boundary [10, 12, 25]. Consistent with camptothecin actions, treatment with NSC in DU-145 cells produced a dose- and time-dependent cell apoptosis accompany with a cell cycle arrest. By using camptothecin-resistant cell lines, DU-145RC0.1 and DU-145RC1, which have a mutated top1 to prevent the binding of camptothecin to the enzyme [22], we have shown that the NSC as well as camptothecin-induced decreases in viable cell numbers were completely blocked by the mutation of top1. Taken together, these data suggest that similar to camptothecin, NSC-induced cell apoptosis and inhibition of cell growth is mediated primary through the interaction with top1, an activation of mitochondrial apoptotic pathway, and an induction of cell cycle arrest. Whether NSC possesses distinct actions from other camptothecin analogs in prostate cancer cells remains to be determined. DNA damage-induced cell apoptosis generally involves the intrinsic apoptotic pathway, in which the mitochondrion plays a central role [10, 26, 27]. The involvement of mitochondria in NSC-induced apoptosis is supported by the demonstration of NSC induction of cyto-chrome ***c*** release from mitochondria to cytosol (Fig. 5c). This is also supported by a previous study showing that NSC causes a loss of mitochondrial transmembrane potential [14]. The observation that NSC-induced Bax and Bak, two pro-apoptotic proteins that can create pores in mitochondrial membranes and promote cytochrome *c* release [28, 29], provides additional evidence to support the involvement of mitochondria in NSC actions. The release of cytochrome ***c*** from mitochondria into cytosol triggers the oligomerization of Apaf-1, resulting in an activation of pro-caspase 9, caspase-3 and/or caspase-7, and eventually cell apoptosis. The dependency of caspase activation in NSC-induced cell apoptosis is supported by the demonstration that NSC-induced caspase 3/7 activity and cell apoptosis were blocked by the concomitant administration of Z-VAD-FMK, a specific pan-caspase inhibitor.

Previous studies in leukemic cells have shown that NSC-induced cell apoptosis and growth inhibition involves the activation of PKCδ activity—an event upstream to mitochondrial trans-membrane potential loss and caspase-3 activation since rottlerin, a specific PKCδ

inhibitor, completely blocked NSC-induced mitochondrial trans-membrane potential loss and caspase-3 activation [14]. However, our current demonstration that concomitant administration of rottlerin, a specific PKCδ inhibitor [21] failed to inhibit NSC-induced cell apoptosis (Fig. 3), modulate caspase activation (Fig. 4) and growth inhibition (Fig. 6), suggests that PKCδ activation is not necessary for NSC-induced cell apoptosis and growth inhibition in DU-145 cells. Furthermore, treatment with rottlerin alone in DU-145 cells produced a dose-dependent decrease in viable cell numbers (Fig. 6), and an increase in cell death (Fig. 3k), a phenomenon observed in other cells such as chronic lymphocytic leukemia cells [30], suggesting that the endogenous PKCδ activity may be necessary for cell survival and/or proliferation. Taken together, these data indicate that NSC actions involve differential molecular targets in different cells, and further support the concept that the effects of PKCδ are highly relevant to cellular context, which may be mediated via distinct pathways [31].

In summary, our current study demonstrates that NSC, a camptothecin analog promoted cell apoptosis and inhibited cell growth in multiple prostate cancer cells. Like camptothecin, the NSC-induced cell apoptosis and growth inhibition may involve the interaction with top1, cell cycle arrest and the activation of mitochondrial apoptotic pathway. These data suggest that NSC is a potential agent for the treatment of prostate cancer, especially hormone-independent prostate cancer and warrants further investigations as NSC possesses antitumor activity, and is superior to topotecan and irinotecan both in vitro leukemic cell cultures and in vivo leukemic animal models [32].

Acknowledgments

We are very grateful to Dr. Robert Schultz at the Drug Synthesis and Chemistry Branch, Developmental Therapeutic Program, Division of Cancer Treatment and Diagnosis, National Cancer Institute Bethesda, MD to provide us the NSC compound; to Dr. Yves Pommier in Laboratory of Molecular Pharmacology, Division of Basic Sciences, National Cancer Institute, Bethesda, MD, USA for the RC1 and RC0.1 cells. This study is partially supported by a NIH grant S/C2P30 CA29502 to YSZ. Y Qiao is supported by a NIH training grant (T32 DK-07313) directed by JIM.

Abbreviations

NSC	NSC606985
PKCδ	Protein kinase Cδ
VBT	Vinblastine
Z-VAD-FMK	Z-VAD-fluoromethylketone
Top1	Topoisomerase 1
VEGF	Vascular endothelial growth factor
HIF-1	Hypoxia-inducible factor 1
FBS	Fetal bovine serum

References

1. Carter HB, Coffey DS. The prostate: an increasing medical problem. Prostate. 1990; 16:39–48. [PubMed: 1689482]
2. Weir HK, Thun MJ, Hankey BF, Ries LA, Howe HL, Wingo PA, Jemal A, Ward E, Anderson RN, Edwards BK. Annual report to the nation on the status of cancer, 1975–2000, featuring the uses of surveillance data for cancer prevention and control. J Natl Cancer Inst. 2003; 95:1276–1299. [PubMed: 12953083]

3. Jemal A, Siegel R, Ward E, Murray T, Xu J, Thun MJ. Cancer statistics, 2007. CA Cancer J Clin. 2007; 57:43–66. [PubMed: 17237035]
4. Rinker-Schaeffer CW, Partin AW, Isaacs WB, Coffey DS, Isaacs JT. Molecular and cellular changes associated with the acquisition of metastatic ability by prostatic cancer cells. Prostate. 1994; 25:249–265. [PubMed: 7971516]
5. Dowling AJ, Tannock IF. Systemic treatment for prostate cancer. Cancer Treat Rev. 1998; 24:283–301. [PubMed: 9805508]
6. Raghavan D, Koczwara B, Javle M. Evolving strategies of cytotoxic chemotherapy for advanced prostate cancer. Eur J Cancer. 1997; 33:566–574. [PubMed: 9274436]
7. Petrylak DP, Tangen CM, Hussain MH, Lara PN Jr, Jones JA, Taplin ME, Burch PA, Berry D, Moinpour C, Kohli M, Benson MC, Small EJ, et al. Docetaxel and estramustine compared with mitoxantrone and prednisone for advanced refractory prostate cancer. N Engl J Med. 2004; 351:1513–1520. [PubMed: 15470214]
8. Tannock IF, de Wit R, Berry WR, Horti J, Pluzanska A, Chi KN, Oudard S, Theodore C, James ND, Turesson I, Rosenthal MA, Eisenberger MA. Docetaxel plus prednisone or mitoxantrone plus prednisone for advanced prostate cancer. N Engl J Med. 2004; 351:1502–1512. [PubMed: 15470213]
9. Wall ME. Camptothecin and taxol: discovery to clinic. Med Res Rev. 1998; 18:299–314. [PubMed: 9735871]
10. Pommier Y, Pourquier P, Fan Y, Strumberg D. Mechanism of action of eukaryotic DNA topoisomerase I and drugs targeted to the enzyme. Biochim Biophys Acta. 1998; 1400:83–105. [PubMed: 9748515]
11. Pizzolato JF, Saltz LB. The camptothecins. Lancet. 2003; 361:2235–2242. [PubMed: 12842380]
12. Pommier Y. Topoisomerase I inhibitors: camptothecins and beyond. Nat Rev Cancer. 2006; 6:789–802. [PubMed: 16990856]
13. Rapisarda A, Uranchimeg B, Scudiero DA, Selby M, Sausville EA, Shoemaker RH, Melillo G. Identification of small molecule inhibitors of hypoxia-inducible factor 1 transcriptional activation pathway. Cancer Res. 2002; 62:4316–4324. [PubMed: 12154035]
14. Song MG, Gao SM, Du KM, Xu M, Yu Y, Zhou YH, Wang Q, Chen Z, Zhu YS, Chen GQ. Nanomolar concentration of NSC606985, a camptothecin analog, induces leukemic-cell apoptosis through protein kinase Cdelta-dependent mechanisms. Blood. 2005; 105:3714–3721. [PubMed: 15671440]
15. Zhu YS, Huang Y, Cai LQ, Zhu J, Duan Q, Duan Y, Imperato-McGinley J. A Chinese medicinal herbal formula ZYD88 inhibits cell growth and promotes cell apoptosis in prostatic tumor cells. Oncology Reports. 2003; 10:1633–1639. [PubMed: 12883751]
16. Hou DX, Tong X, Terahara N, Luo D, Fujii M. Delphinidin 3-sambubioside, a Hibiscus anthocyanin, induces apoptosis in human leukemia cells through reactive oxygen species-mediated mitochondrial pathway. Arch Biochem Biophys. 2005; 440:101–109. [PubMed: 16018963]
17. Zhu YS, Pfaff DW. Differential regulation of AP–1 DNA binding activity in rat hypothalamus and pituitary by estrogen. Mol Brain Res. 1998; 55:115–125. [PubMed: 9645966]
18. Baydas G, Reiter RJ, Akbulut M, Tuzcu M, Tamer S. Melatonin inhibits neural apoptosis induced by homocysteine in hippocampus of rats via inhibition of cytochrome *c* translocation and caspase–3 activation and by regulating pro- and anti-apoptotic protein levels. Neuroscience. 2005; 135:879–886. [PubMed: 16213988]
19. Kumi-Diaka J, Sanderson NA, Hall A. The mediating role of caspase-3 protease in the intracellular mechanism of genistein-induced apoptosis in human prostatic carcinoma cell lines, DU145 and LNCaP. Biol Cell. 2000; 92:595–604. [PubMed: 11374438]
20. Lu KH, Lue KH, Liao HH, Lin KL, Chung JG. Induction of caspase-3-dependent apoptosis in human leukemia HL-60 cells by paclitaxel. Clin Chim Acta. 2005; 357:65–73. [PubMed: 15963795]
21. Matassa AA, Carpenter L, Biden TJ, Humphries MJ, Reyland ME. PKCdelta is required for mitochondrial-dependent apoptosis in salivary epithelial cells. J Biol Chem. 2001; 276:29719–29728. [PubMed: 11369761]

22. Urasaki Y, Laco GS, Pourquier P, Takebayashi Y, Kohlhagen G, Gioffre C, Zhang H, Chatterjee D, Pantazis P, Pommier Y. Characterization of a novel topoisomerase I mutation from a camptothecin-resistant human prostate cancer cell line. Cancer Res. 2001; 61:1964–1969. [PubMed: 11280753]
23. Beppu K, Nakamura K, Linehan WM, Rapisarda A, Thiele CJ. Topotecan blocks hypoxia-inducible factor-1alpha and vascular endothelial growth factor expression induced by insulin-like growth factor-I in neuroblastoma cells. Cancer Res. 2005; 65:4775–4781. [PubMed: 15930297]
24. Saleem A, Edwards TK, Rasheed Z, Rubin EH. Mechanisms of resistance to camptothecins. Ann N Y Acad Sci. 2000; 922:46–55. [PubMed: 11193924]
25. Soe K, Rockstroh A, Schache P, Grosse F. The human topo-isomerase I damage response plays a role in apoptosis. DNA Repair (Amst). 2004; 3:387–393. [PubMed: 15010314]
26. Jiang X, Wang X. Cytochrome *c*-mediated apoptosis. Annu Rev Biochem. 2004; 73:87–106. [PubMed: 15189137]
27. Norbury CJ, Zhivotovsky B. DNA damage-induced apoptosis. Oncogene. 2004; 23:2797–2808. [PubMed: 15077143]
28. Adams JM, Cory S. The Bcl-2 protein family: arbiters of cell survival. Science. 1998; 281:1322–1326. [PubMed: 9735050]
29. Reed JC. Bcl-2 family proteins. Oncogene. 1998; 17:3225–3236. [PubMed: 9916985]
30. Ringshausen I, Oelsner M, Weick K, Bogner C, Peschel C, Decker T. Mechanisms of apoptosis-induction by rottlerin: therapeutic implications for B-CLL. Leukemia. 2006; 20:514–520. [PubMed: 16437144]
31. Yang C, Kazanietz MG. Divergence and complexities in DAG signaling: looking beyond PKC. Trends Pharmacol Sci. 2003; 24:602–608. [PubMed: 14607084]
32. Liu W, Zhu YS, Guo M, Yu Y, Chen GQ. Therapeutic efficacy of NSC606985, a novel camptothecin analog, in a mouse model of acute promyelocytic leukemia. Leuk Res. 2007; 31:1565–1574. [PubMed: 17428537]

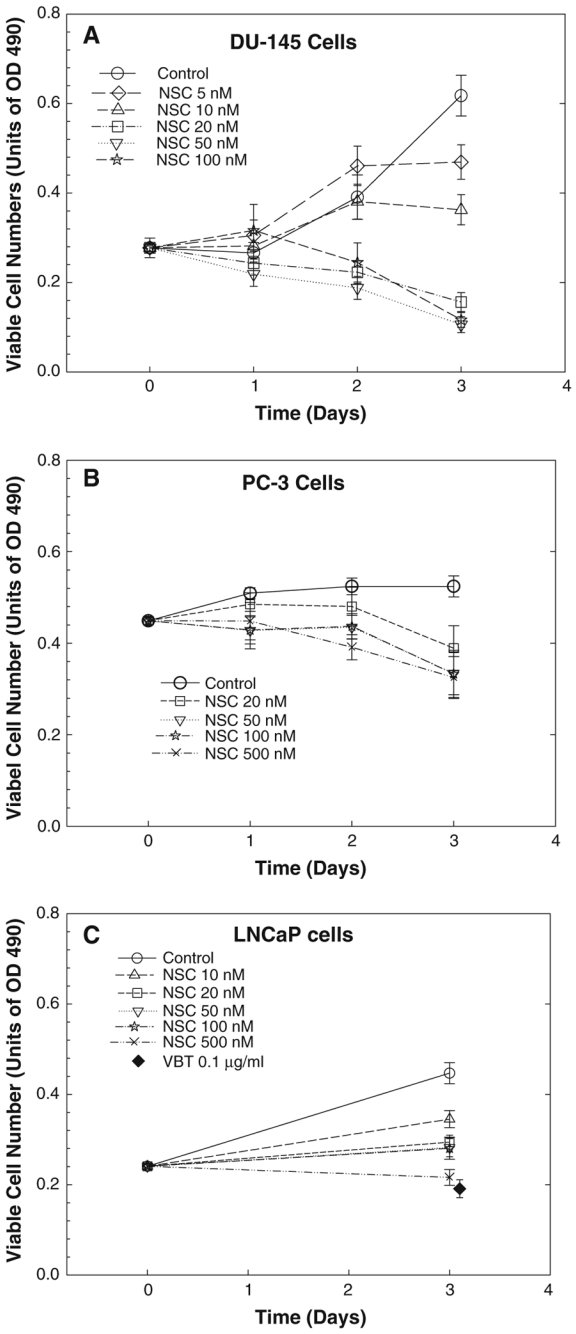

Fig. 1.

NSC decreased the viable cell numbers in DU-145 (**a**), PC-3 (**b**) and LNCaP(**c**) prostate cancer cells. Cells were treated with various doses of NSC for different times as indicated. The number of viable cells was determined as described in “Materials and methods”. The data are presented as units of absorbance at 490 nm (OD490), and the values are the mean ± SEM of six to nine individual samples from two to three independent triplicate experiments. Treatment with vinblastine (*VBT*) at 0.1 μg/ml was used as a positive control

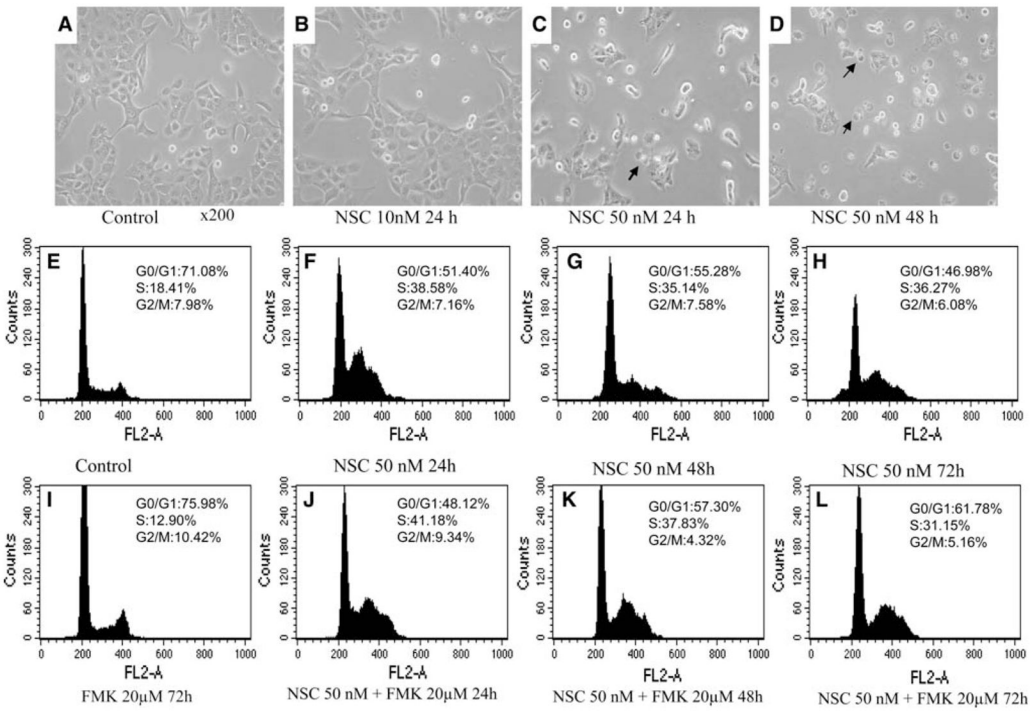

Fig. 2.

The effect of NSC on cell morphology and DNA distribution in DU-145 cells. **a**–**d** Representative photographs of NSC treatment for 24 or 48 h in DU-145 cells. The original images were taken under an inverted microscope with an objective lens ×20. Apoptotic cells are pointed by arrows. Panels E–H are flow cytometric analysis of nuclear DNA distribution in DU-145 cells treated with or without NSC (50 nM) for 24, 48, and 72 h in the presence or absence of 20 μM of Z-VAD-FMK (FMK)

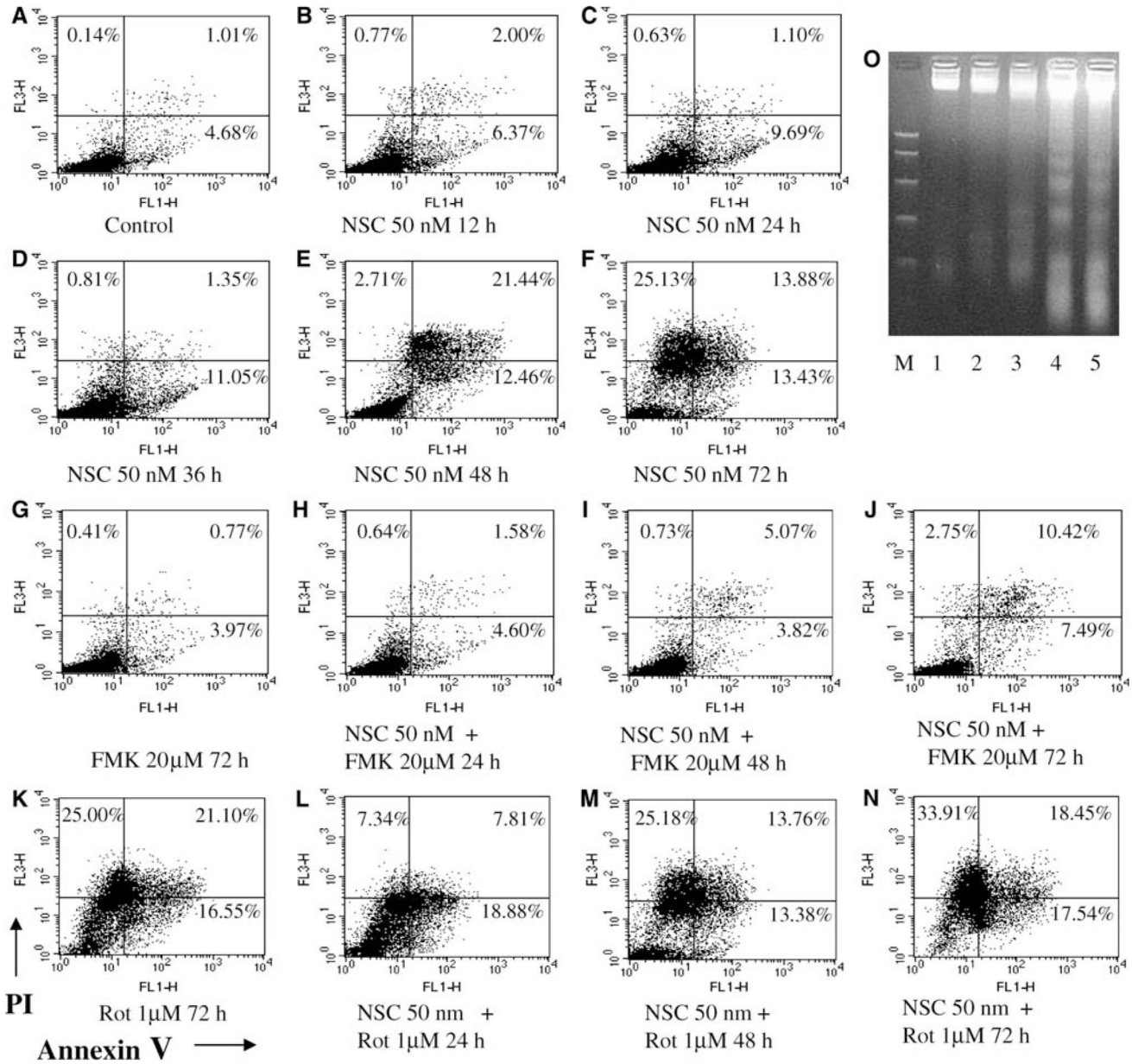

Fig. 3.

NSC promoted cell apoptosis in DU-145 cells. **a**–**n** Flow cytometric analysis of apoptosis with Annexin-V/propidium iodide (*PI*) staining as described in "Materials and methods". DU-145 cells were treated with or without NSC (50 nM) for various times in the presence or absence of Z-VAD-FMK (FMK, 20 μM) or rottlerin (Rot, 1 μM) as indicated. Cells located in the lower left quadrant that are viable are Annexin V and PI negative (Annexin V^-/PI^-); cells located in the lower right quadrant that are in early apoptosis are Annexin V positive and PI negative (Annexin V^+/PI^-); Cells located in the upper right quadrant that are in late apoptosis or in secondary necrosis are both Annexin V and PI positive (Annexin V^+/PI^+); and cells in upper left quadrant that are in isolated nuclei, or in late necrosis, or cellular debris are Annexin V negative and PI positive (Annexin V^-/PI^+). Panel O shows the NSC induced DNA fragmentation in DU-145 cells. Lane M devotes DNA size markers in kilobases 1,000, 700, 500, 300, 150, and 50 from top to bottom. *Lane 1* is DU-145 control,

lane 2 DU-145 cells without NSC treatment for 24 h, *lanes 3–5* DU-145 cells treated with NSC (50 nM) for 24, 48 and 72 h, respectively

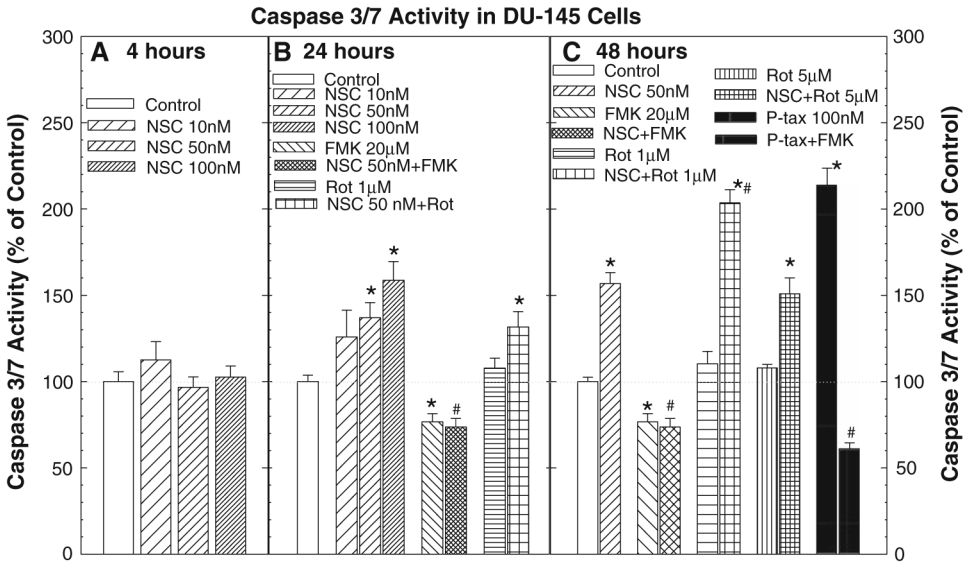

Fig. 4.

NSC produced a dose- and time-dependent induction of caspase activity in DU-145 cells: DU-145 cells were treated with or without various doses of NSC for the indicated times, and the caspase 3/7 activity was determined as described in the “Materials and methods”. The data were presented as percent of vehicle control, and the values are the mean ± SEM of six to nine individual samples from two to three independent triplicate experiments. **P* < 0.05 and ***P* < 0.01 compared to vehicle control; #*P* < 0.05 and ##*P* < 0.01 compared to 50 nM NSC treatment (Student-Newman–Keuls test). Ptax devotes paclitaxel, FMK, Z-VAD-FMK and Rot, rottlerin

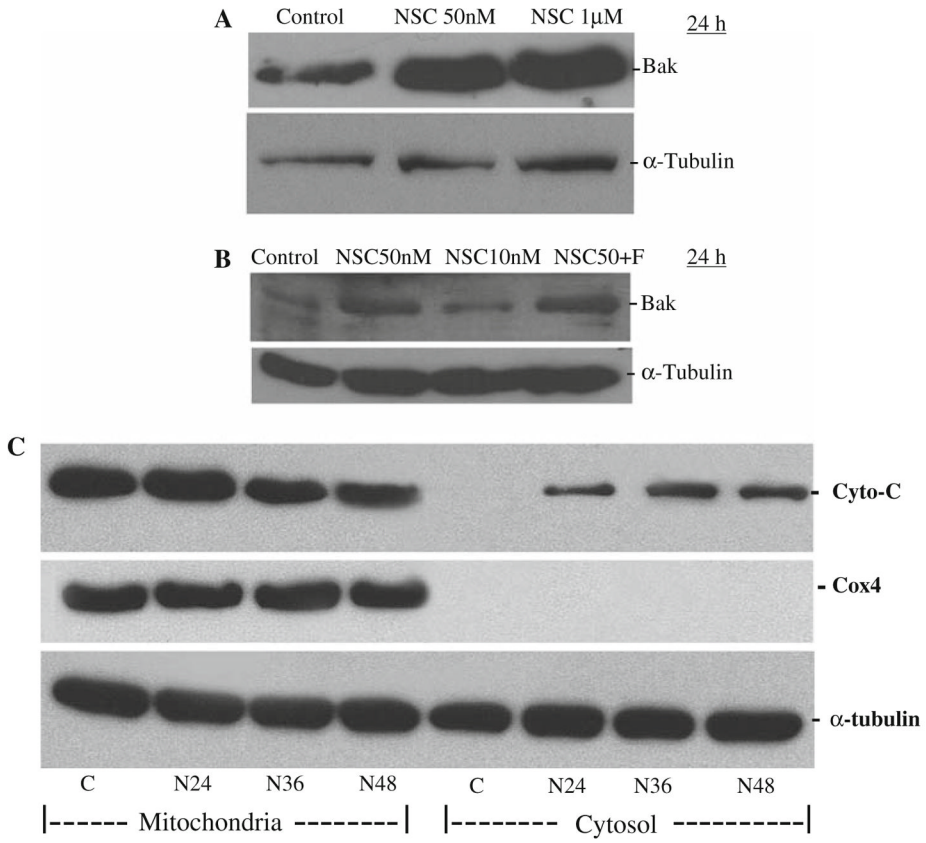

Fig. 5.

NSC treatment increased Bax (**a**) and Bak (**b**) levels and induced cytochrome *c* release from mitochondria to cytosol (**c**) in DU-145 cells. Cells were treated with various doses of NSC for 24 h (**a**, **b**), or 50 nM of NSC (*N*) for various times (**c**) as indicated. The levels of Bax and Bak and the release of cytochrome *c* from mitochondria to cytosol were analyzed by Western blot with specific antibodies as described in “Materials and methods”. *F* devotes Z-VAD-FMK (20 μM), a pan-caspase inhibitor, which was co-administrated with 50 nM of NSC for 24 h

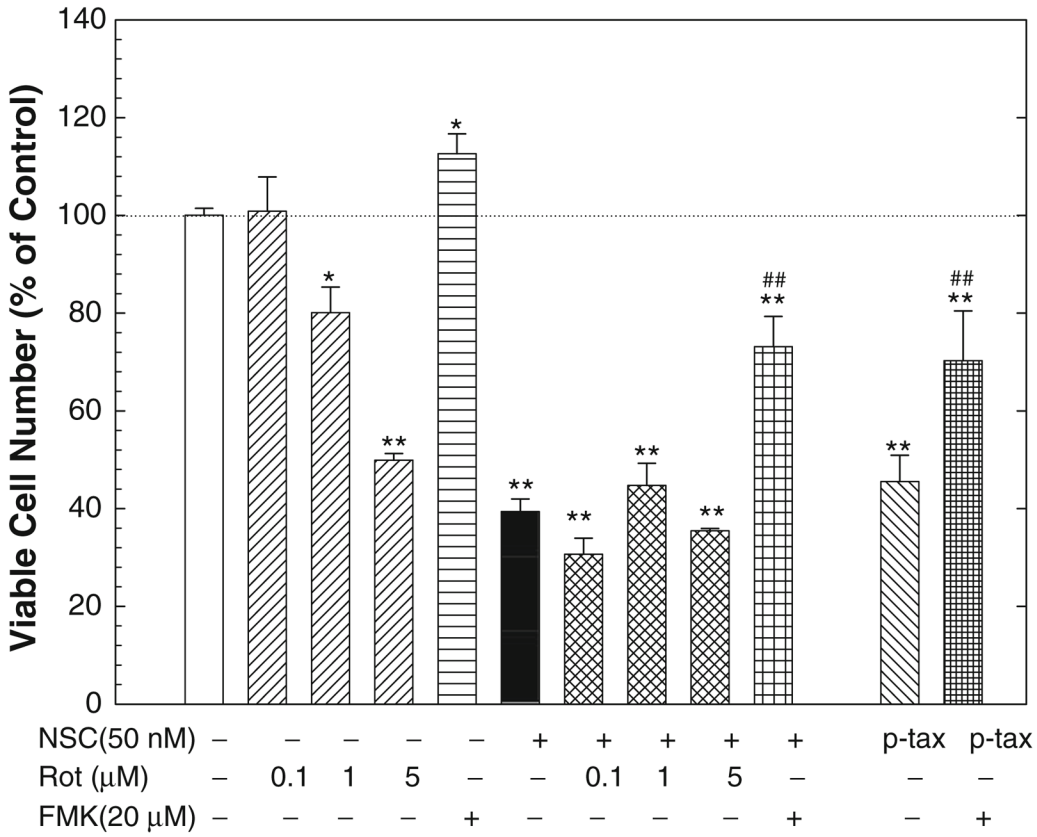

Fig. 6.

The NSC-induced decrease in viable cell number was blocked by Z-VAD-FMK, a pan-caspase inhibitor, but not rottlerin, a PKCδ inhibitor in DU-145 cells. DU-145 cells were treated with or without NSC (50 nM) for 72 h in the presence or absence of various doses of rottlerin or 20 μM of Z-VAD-FMK, and the numbers of viable cells were determined as described in “Materials and methods”. The data were presented as percent of vehicle control, and the values are the mean ± SEM of 6–12 individual samples from two to four independent triplicate experiments. * $P < 0.05$ and ** $P < 0.01$ compared to vehicle control; ## $P < 0.01$ compared to 50 nM NSC treatment (Student-Newman–Keuls test). P-tax devotes paclitaxel (100 nM), FMK, Z-VAD-FMK and Rot, rottlerin

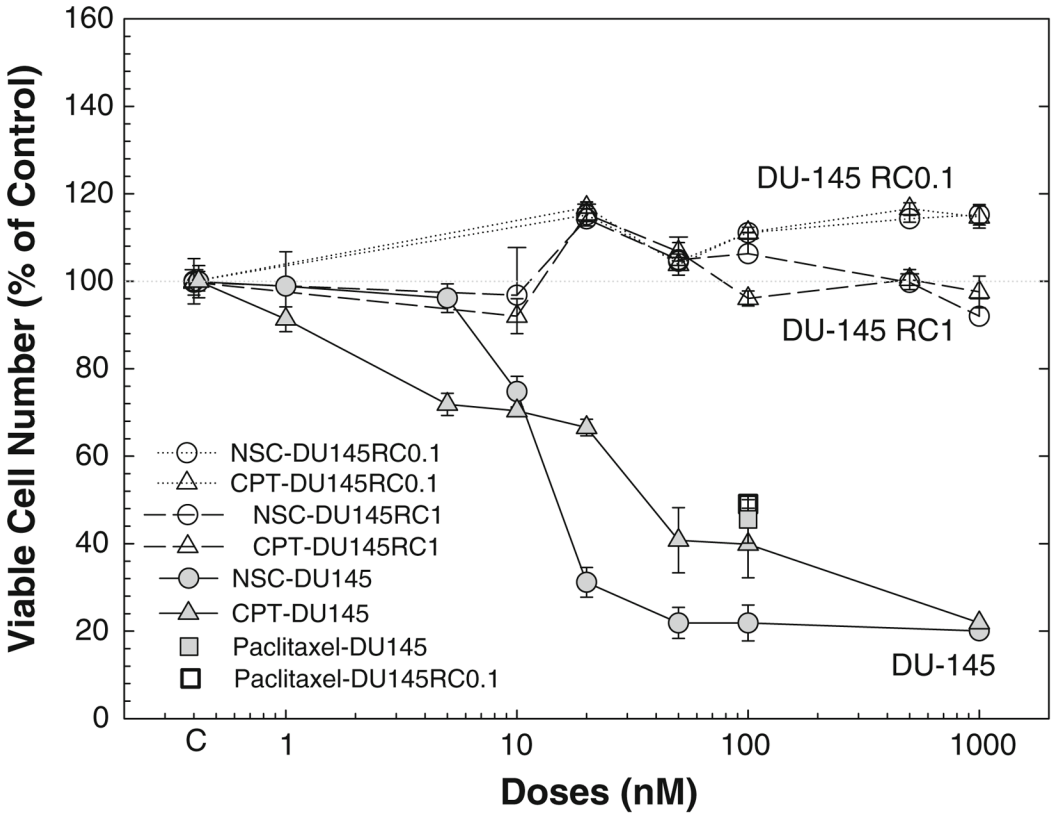

Fig. 7.

Mutation of top1 in DU-145 cells blocked NSC-induced decrease in viable cell numbers: DU-145, DU-145RC0.1 and DU-145RC1 cells were treated with or without various doses of NSC or camptothecin (CPT) for 72 h, and the numbers of viable cells were determined as described in “Materials and methods”. The data were presented as percent of vehicle control, and the values are the mean ± SEM of 6–12 individual samples from 2–4 independent triplicate experiments